STUDY ON PLUME CHARACTERISTICS OF PULSED PLASMA THRUSTER[*†]

Kentaro Kawahara[‡], Naoki Kumagai[§], Kensuke Sato[‡], Kohji Tamura[§], Takahiro Koide[‡], Kenji Harima[¶], Tadanori Fukushima[¶], Haruki Takegahara[#]

Tokyo Metropolitan Institute of Technology, Department of Aerospace Engineering

Asahigaoka 6-6, Hino, Tokyo, 191-0065, JAPAN

+81-42-585-8659

ppt@astak3.tmit.ac.jp

IEPC-03-0160

Abstract

The plume characteristics of TMIT-PPT for μ-Lab Sat II were investigated. In this paper, five contents about 1) the high speed camera experiment, 2) the effect of the opening angle of hood on the PPT performance, 3) the plume expansion without hood, 4) to confirm the thrust direction, and 5) the effect of self-induced magnetic field are described. As the high speed camera experiment, we could observe the restrike and quasi-steady state of the discharge current. As a result of changing the hood angle, the performance of PPT with 0˚ hood is the lowest, compared with the other hood angles (15˚, 30˚, 45˚, 60˚ and without hood). The reason was the decrease of kinetic energy of the charged particle in plume because of the collision with the hood wall. And, after 500,000 shots operation with 2.3 J/shot without hood, the aluminum plate 1100 mm away from the thruster were contaminated uniformly. However, the change of sample mass arranged on the aluminum plate was too small to measure. And, as a result of the preliminary inspection of the contamination, carbon was dominant and the proportion of the constituent elements were not different between near and far point from the thrust axis. In the experiment to confirm the thrust direction, the plume inclination was confirmed from the photograph. As a result of changing the angle of line between thruster head and capacitor, as the angle of line increase, axial impulse bit had a tendency to decrease and mass shot had a tendency to increase.

Introduction

Because the tendency of satellite design to be towards small and low cost, the need for miniaturizing the propulsion systems have become apparent. Pulsed Plasma Thruster (PPT) is one of the promising propulsion system for attitude control, station keeping, de-orbit, formation flying, and drag compensation of the small, micro- and nano-satellite because of the following reasons.

1) Simplicity.
   No tankage, seals nor mechanical valves.
2) Light weight and high reliability.
   Only two power supplies.
   : Capacitor charge power supply and ignition power supply.
   Only one moving device.
   : Solid propellant feed mechanism to discharge chamber.
3) Small impulse bit (impulse per shot) level.
   Precise total impulse control.

---

[*] Presented as Paper IEPC-03-0160 at the 28th Internatinal Electric Propulsion Conference, Toulouse, France, 17-21 March 2003.

[‡] Graduate Student.

[§] Graduate Student, Student Member AIAA.

[¶] Under Graduate Student.

[#] Professor, Senior Member AIAA.

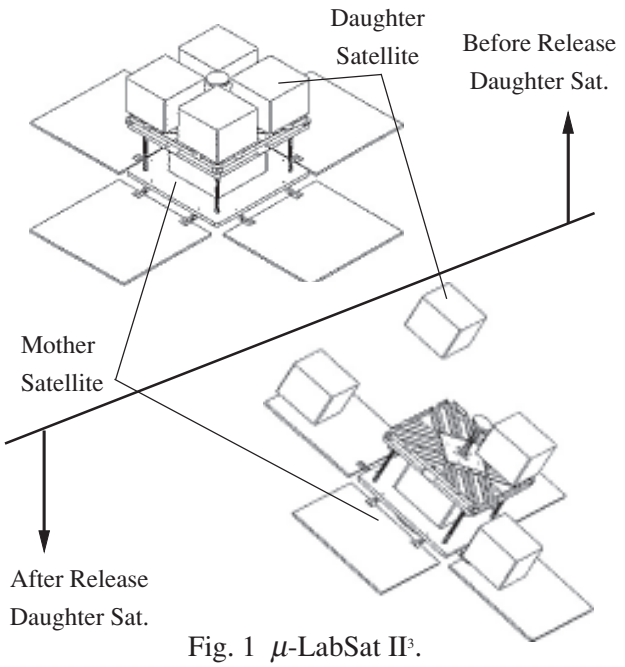

Fig. 1 μ-LabSat II[3].

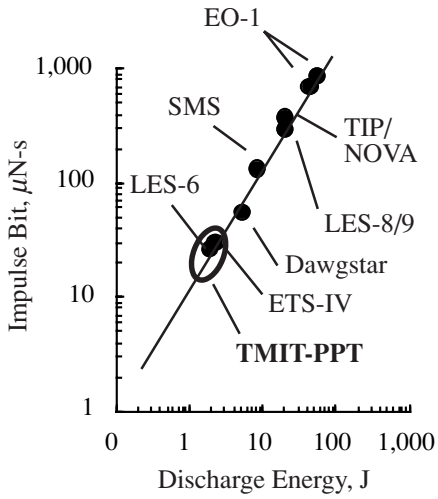

Fig. 2 Target of TMIT-PPT and Flowing PPTs[4-8].

Considering these advantageous characteristics and requirements of small satellites, TMIT have performed R&D for application of PPT to small satellite, μ-Lab Sat II in collaboration with NASDA[1-3].

μ-Lab Sat II is a 50kg-class piggyback satellite, and consist of 1 mother satellite and 4 daughter satellites as shown in Fig. 1. μ-Lab Sat II requires light weight and low power consumption to the propulsion system and Fig. 2 shows the target of TMIT-PPT impulse bit versus energy compared with the past and flowing PPTs[4-8]. TMIT-PPT is one of the lowest energy level PPT.

Now, we have transposed from the BBM phase to the EM phase[1, 2].

Vacuum Facility

All experiments were performed in the vacuum chamber (1 m diam., 1.8 m length) with two turbo-molecular pumping systems (2,000 L/s ¥ 2 EA), a mechanical booster pumping system and a rotary pumping system. Its degree of vacuum was maintained in the range of 10^{-4} Pa (10^{-6}Torr) during each PPT operation.

High Speed Camera Experiment

Compared with the coaxial PPT, the rectangular PPT may generate off-axis thrust component because of it's configuration. For example, the plume asymmetric distribution in the perpendicular plane to the electrodes of rectangular PPT was reported[9-10]. For the purpose of mounting TMIT-PPT to μ-Lab Sat II, it is important to evaluate the plume distribution and off-axis thrust vector. So, high speed camera was used to observe the behavior of the discharge current.

Figure 3 shows the configuration of high speed camera experiment. There are two power supplies, one is the main power supply and the other is the ignition power supply. Ignition power carries the signal which indicate the timing of ignition to the pulse generator. The pulse generator can delay and amplify the ignition monitor signals, and carries these signals to the high speed camera. As soon as the pulse generator carries the signal to the high speed camera, it starts to take eight images and carries signals which indicate the timing of taking images to a oscilloscope. At the same time, the main discharge current waveform is measured by the Rogowski coil and carries it to the oscilloscope. Compared the main discharge current waveform with the signal from high speed camera, it is obvious when the images were taken by the high speed camera.

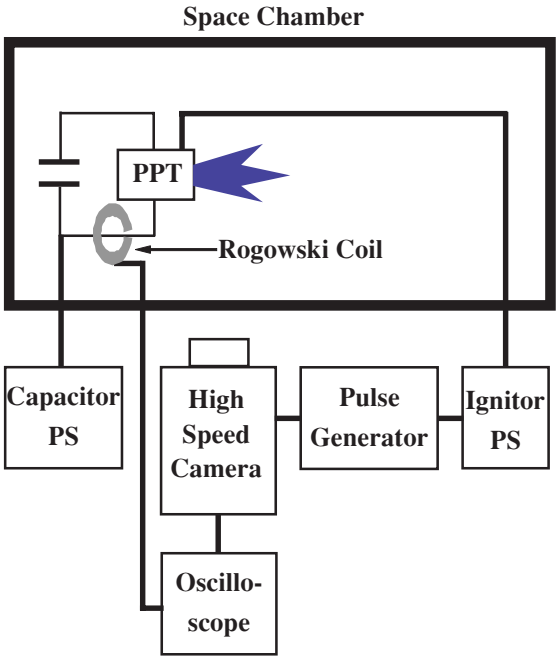

Fig. 3 Experimental Apparatus of High Speed Camera Experiment.

Table.1 Performance of ULTRA 8.

Frame Rates	**1,000 - 100,000,000 pps**
Exposure Times	**10ns - 1ms (10ns step)**
Photography Number	**8 images**
Delay to 1st exposure	**90ns - 10ms (10ns step)**
Spectral Response	**380nm - 850 nm**
Dynamic Range	**12 bit**

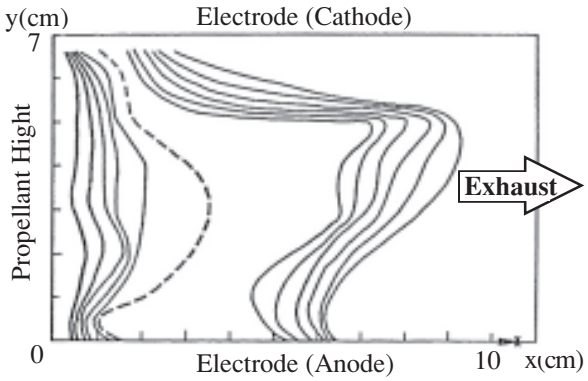

Fig. 5 Current Distribution Measured with a Small Rogowski Coil at the Current Reversal. (AFOSR-TR-77-0623 by Palumbo and Begun[9])

The high speed camera used in this experiment is "ULTRA8" made by NAC Image Technology. As shown in Table 1, ULTRA8 can take eight images at a rate of up to 100,000,000 pps and provides up to eight images as digital format.

Figure 4 shows the image of discharge, provided that the frame rate was set to 4,000,000 pps and the exposure time for each image was 20ns. As shown Fig. 4 b), the spike indicates the timing of taking the image. The images taken at the spike number from #1 to #8 and from #9 to #16 provide the different discharge. But we can consider that these are successive images during a single pulse because these discharge image has a repeatability.

As shown Fig. 4 c), #5 indicates that the arc discharge occurred at the surface of Teflon propellant. This phenomenon was shown in the other high speed photographs reported by Vondra, et al[11,12].

After image #5, two luminous flow (downstream luminous flow) were generated at the anode and cathode separately and they were mixed at the vicinity of the cathode and moved to the downstream (image #7 - #13). At the same time, another luminous flow (upstream luminous flow) occurred at the surface of Teflon propellant. These flows indicated "restrike mode". However, the downstream luminous flow looked like remaining at tip of the electrode (image #10 - #13). This phenomenon was different from the opinion that the current sheet might move to the downstream.

The observed slight luminous flow at the upstream indicated the first current reversal as reported by Palumbo and Begun (image #13 - #14)[9]. Furthermore they measured the current distribution between the electrodes gaps using a small Rogowski coil, and confirmed that there are two separate current paths which were formed as a result of the reversal of the current direction within the plasma as shown in Fig. 5 in this page[9]. In this figure, the solid contours on either side indicate the extremities of various percentages of the total reverse current flow. Between x = 0 and the dashed line, the first solid contour shows 50% of the total and each subsequent line includes 10% more. To the right of the dashed line the first solid contour shows 50% and each subsequent line 10% less net current flow. Compared with Fig. 5 and image #13,#14 of Fig. 4, the discharge current distribution between the electrodes agreed well with the luminous flows except the downstream luminous flow in the vicinity of the cathode. In Fig. 5, it wasn't confirmed the luminously mixture at the downstream region shown in our image. This difference might be caused by the characteristics of Rogowski coil which could not measure the two current paths separately through their loop. On the other hand, we can think that the luminously mixture at the downstream region might be the quasi-neutral plasma flow, and luminous path might indicate the trajectories of the charged particles.

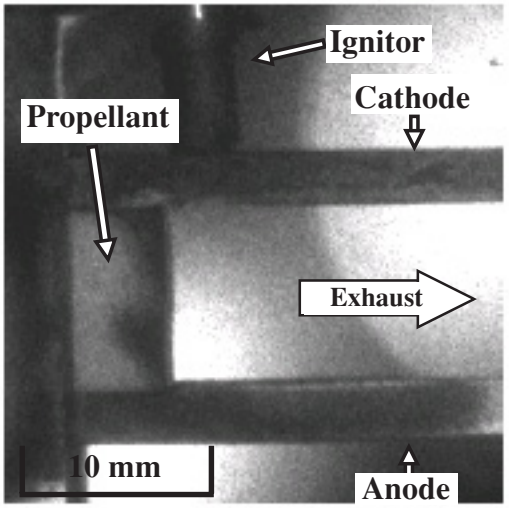

(a) Thruster Configuration.

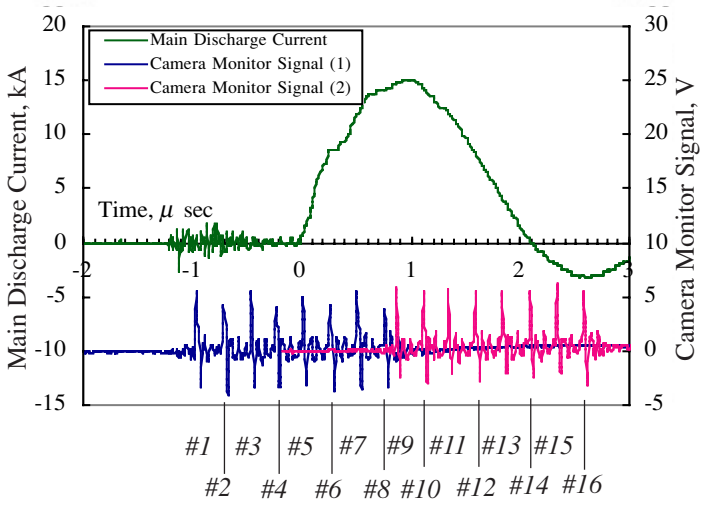

(b) Timing of Taking Images.

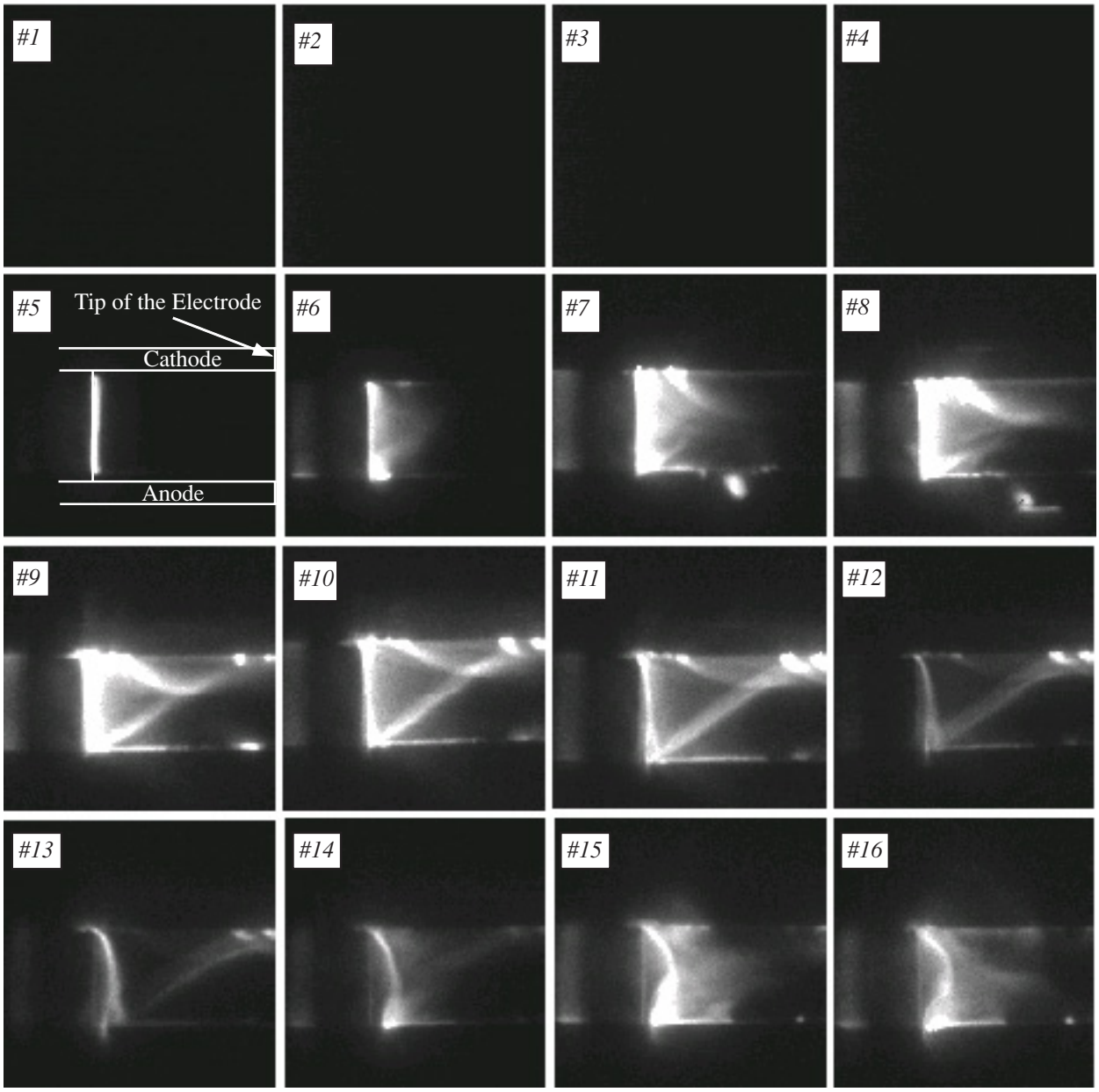

(c) Successive Images of Discharge.

Fig.4 Results of High Speed Camera Experiment.

As shown in image #10 which shows the first current peak, the luminous flow canting from the cathode to anode was about 75˚ and it from the anode to cathode is 65˚. Though these canting angles were quite close to the angle reported by Markusic and Choueiri[13] (about 60˚), the our current appeared to incline in the contrary direction compared with their results. But this reason and the effect of the current sheet canting on the off-axis components of thrust were not obvious now. The off-axis components of thrust will be measured with the target pendulum[14].

Effect of Hood Angle on Performance

It is important for the satellites to narrow down the plume expansion. To prevent the plume expansion, the hood is useful. In this section, the effects of hood angle on performance are shown. We have evaluated the effect of hood angle on the PPT performance with 0˚, 15˚, 30˚, 45˚, 60˚ hoods. Hood angle θ is defined the half vertical angle as shown Fig. 6.

Figure 7 shows the impulse bit, mass shot, and specific impulse of the operation with 0˚, 15˚, 30˚, 45˚, 60˚ hoods and without hood. In these figures, 180˚ angle indicates the value of without hood. In this experiment, we used two electrodes made of Mo and Brass.

As shown Fig. 7 a) , the impulse bit with hoods operation were lower than that without hood operation. The cause of the impulse bit loss with hoods operation was a decline of exhaust velocity due to the collision of particles with the hoods inner wall. And as shown Fig. 7 a), 15˚, 30˚, 45˚, 60˚ hoods operation provided the close impulse bit and mass shot, while 0˚ hood operation did the lowest impulse bit and mass shot in all hoods operation. Because impulse bit decreased more than mass shot, specific impulse of 0˚ hood operation was the lowest in all hoods operation as shown in Fig. 7 b).

Figure 8 shows the photograph of inner wall of 45˚, 60˚ hoods. The color of the wall changed into brown or black due to the contamination of the plume, and the black area was mainly at the center of the hood. It said the charged particle in the plume concentrated near the electrode because the $\boldsymbol{j} \times \boldsymbol{B}$ force was high there. The

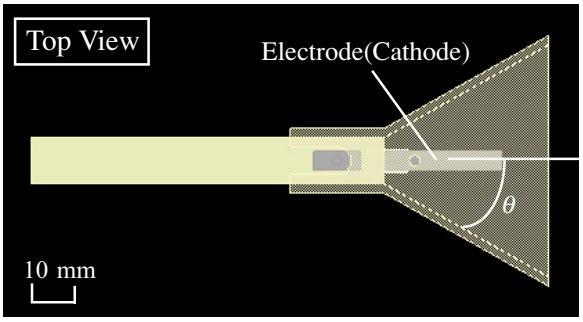

Fig. 6 TMIT-PPT with θ degree Hood.

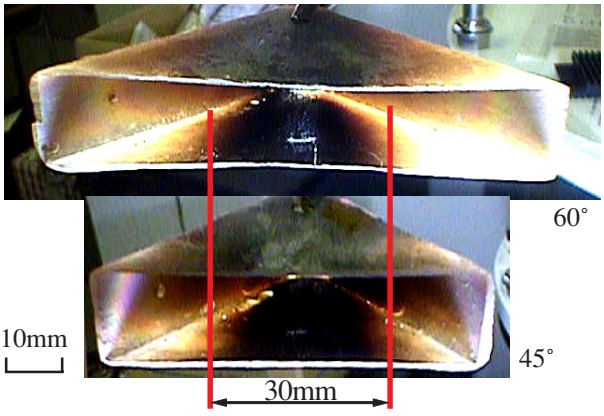

Fig. 8 Plume Contamination to Hood.

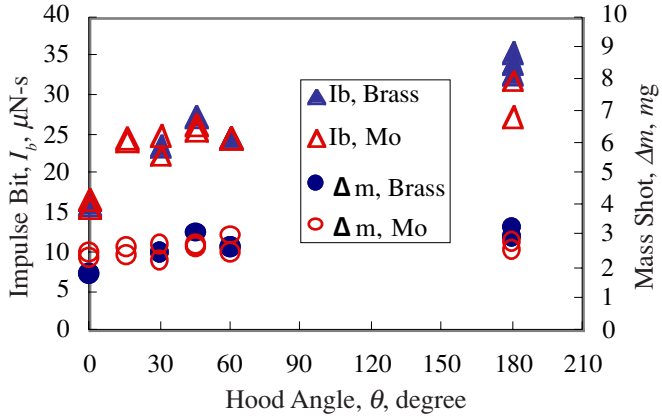

a) Impulse Bit and Mass Shot vs Hood Angle.

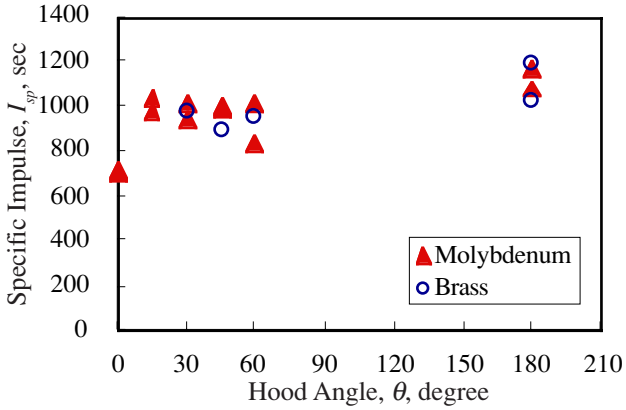

b) Specific Impulse vs Hood Angle.

Fig. 7 The Performance with Hood.

width of the black area at the exit of the hood was about 30mm. This was the same width compared with that of 15˚ hood's exit. It said the charged particle didn't collide with the inner side wall of the 15˚, 30˚, 45˚, 60˚ hoods very often, but with the 0˚ hood the collision of the charged particle and the inner side wall of the hood was occurred. The charged particle lost the kinetic energy by the collision. So impulse bit of 0˚ hoods operation was the lowest in all hoods operation.

In this experiment, it appeared that 15˚, 30˚, 45˚, 60˚ hoods operation provided the close impulse bit and mass shot, and 0˚ hood operation did the lowest impulse bit and mass shot in all hoods. In the experiments of ETS-IV PPT, Hirata and Murakami[15] reported that contamination distribution was constant with over about 40˚ hood and with the hood less than about 40˚, the contamination distribution was narrower than with over about 40˚ hood. And it was reported by Myers and Arrinton[10], the charged particle spread out about 40˚ from exit of the hood and the neutral particle did about 180˚. From these results, 60˚ hood was too large to apply because the hood must prevent more neutral particle in the plume. And the charring was occurred often on the ablation area when used the 15˚ hood. So, we applied 30˚ hood for TMIT-PPT Engineering Model.

Plume Expansion

Generally, the influence of the exhaust plume from the thruster is very important problem because it may have influences to the optical sensor or change the radiation characteristics of the satellite surface. To consider about the PPT, the contamination problem is more severe than the other thrusters because the Teflon which is the propellant of PPT contain carbon. But it was reported[9] the influence of the contamination to the satellite surface was very low because the operation power was very low. However the color of our vacuum chamber wall changed into brown from silver. Therefore, it was decided to evaluate the plume expansion and the contamination of PPT without the hood.

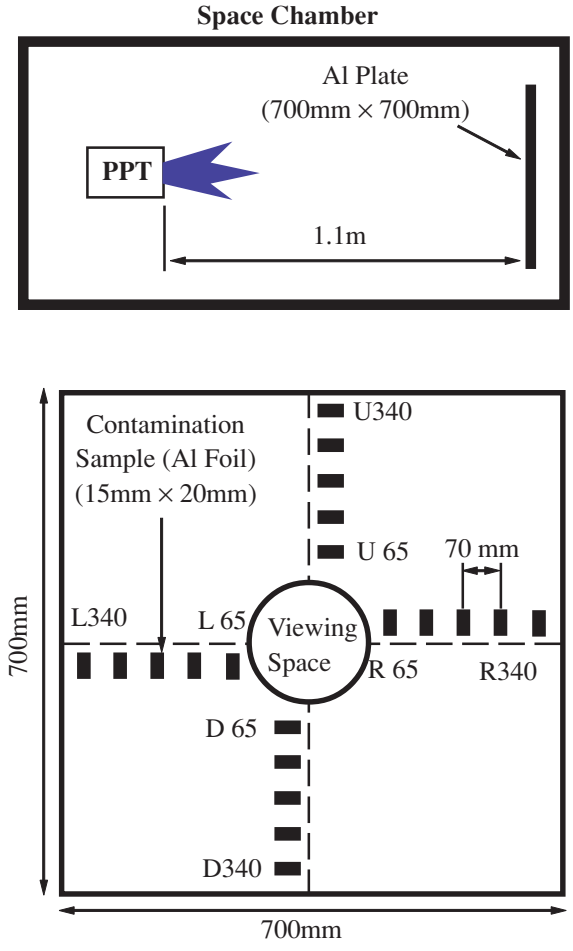

Fig. 9 Experimental Apparatus of Plume Expasion Test without Hood.

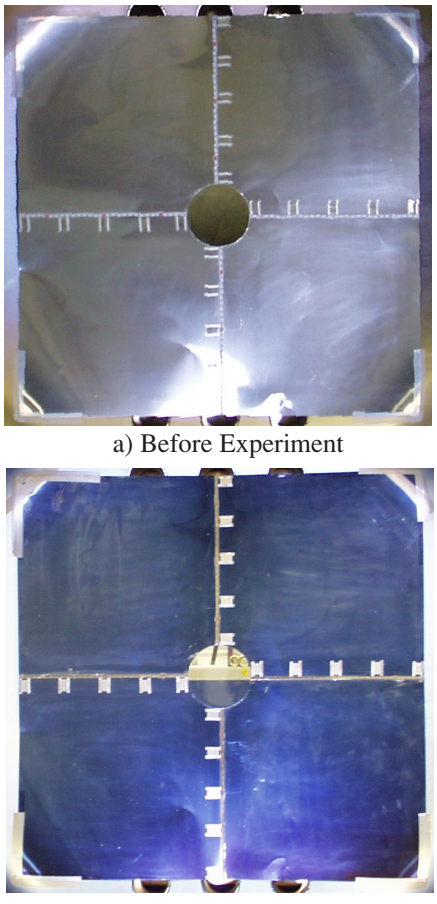

a) Before Experiment

b) After Experiment

Fig. 10 Aluminum Plate

Figure 9 shows the apparatus of the experiment to evaluate the plume expansion without the hood operation. An aluminum plate (700mm × 700mm) was fixed 1.1m away from the thruster. In this aluminum plate, there was 20 contamination samples made by the aluminum foil and those were fixed such as Fig. 9 to evaluate two dimensional distribution of the plume expansion and were spaced every 70mm. After the 500,000shots operation of PPT with 2.3J/shot, and the measurement of the mass of the contamination samples and the preliminary inspection of contamination were conducted.

Figure 10 shows the aluminum plate before and after this experiment. The color of the plate changed into blue from silver. No measurable mass change of the contamination samples were observed with the microbalance which has 0.1mg resolution. As a result, the rate of deposition of the contamination on the samples was at most 0.2 ng/shot.

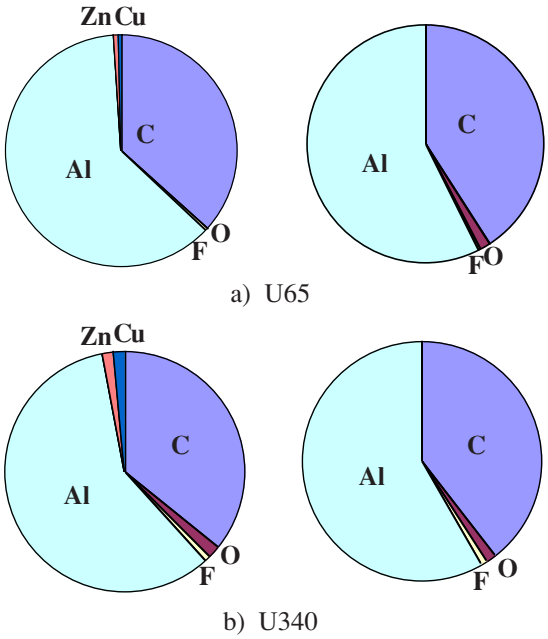

Fig. 11 Mass Ratio of Constituent of Contamination on U65 and U340 Samples.

The preliminary inspection of contamination on U65 and U340 contamination samples was conducted with SEM (Scanning Electron Microscope) and EDX (Energy Dispersive Xray spectrometer). This analysis were conducted at two measurement point on each contamination sample. Figure 11 shows the proportion of constituents of contamination at each measurement point. As shown in these figures, the contamination was almost composed of carbon, and a little copper and zinc from Brass electrodes were observed. Compared U65 with U340, little differences were observed about the proportion of constituent of contamination. Because contamination distribution on the aluminum plate was uniform as described above, the constituents of contamination on the down, right, and left samples are considered to be the same as the upward samples.

Thrust Direction

The thruster is restricted on the weight and size to mount it on the small satellite. So, for the thruster to use the attitude control and de-orbit, it has to be designed to be able to change the thrust direction without using the large area. To change the thrust direction without inclining the thruster, we made the thruster which the electrodes had the 45˚ inclination in the plane perpendicular to the electrodes. We thought 45˚ cant type thruster might generate the 45˚ inclined thrust component compared with straight type thruster.

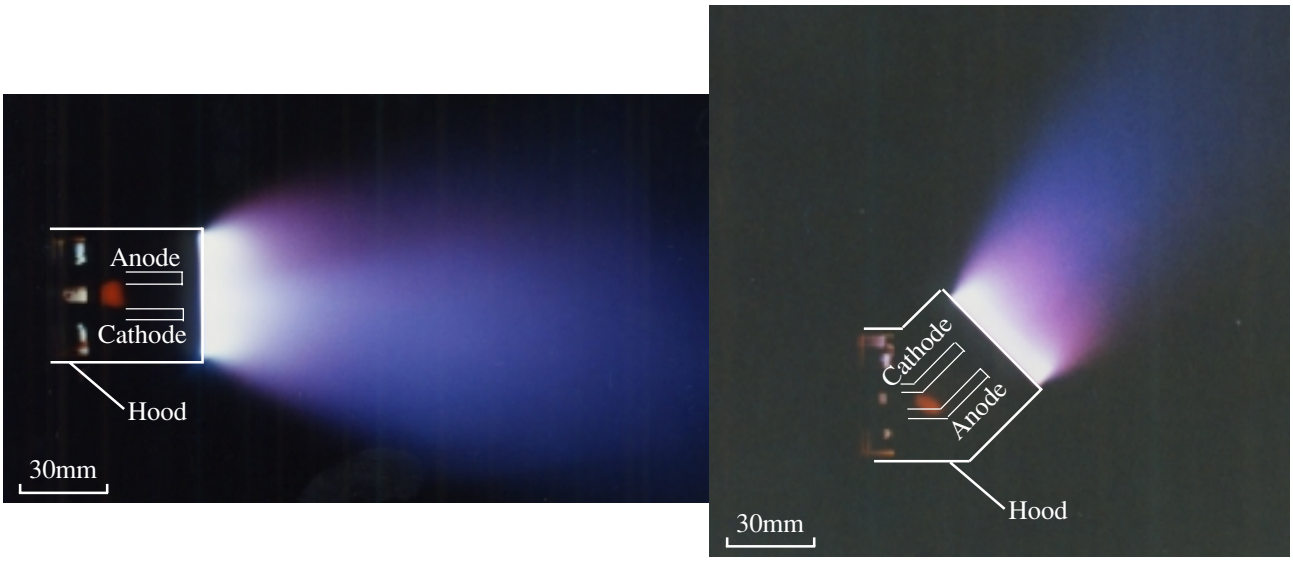

a) The Plume of Straight Type Thruster.

b) The Plume of Cant Type Thruster.

Fig. 12 The Photograph of the Plume.

The performance of this thruster was measured and the inclination of the plume was checked visually.

Figure 12 a), b) shows the photograph of the plume which were exposed 5shot operation. As shown this figure, the plume of cant type thruster had inclination compared with straight type thruster. And the specific impulse of this thruster was about 1000s, this value was approximately the same as that of straight type thruster. In the future, the thrust vector of this thruster will evaluate and check its inclination.

The Effect of Self-Induced Magnetic Field

PPT obtain electromagnetic acceleration by the $\boldsymbol{j}\times\boldsymbol{B}$ force from discharge current between the two electrodes and its self-induced magnetic field. So, the thrust direction and thrust is changed by the direction and strength of the magnetic field. In the rectangular PPT, the magnetic field is generated by the discharge current and it's direction is in parallel plane to the electrodes, then it generates the thrust to the vertical against the ablation area. But in fact, lines between the thruster head and capacitor generates the magnetic field and it may have an influence on that in the discharge chamber.

It is important to evaluate the influence of the self-induced magnetic field generated by the line between the thruster head and capacitor. So, the influence was investigated on the configuration as shown Fig. 13. In this figure, the exhaust direction is y axis. A fulcrum of the line was fixed 6.5mm away from the ablation area. The performance of PPT was measured in the case of changing the line angle 0°, 45°, 90°, 135°, 180° in the order of decreasing the thrust and 225°, 270°, 360° in the order of increasing the thrust.

Figure 14 shows the performance of PPT. As the angle of line increased from 0° to 180°, impulse bit tended to decrease and mass shot tended to increase and as the angle of line increased from 180° to 360°, impulse bit tended to increase and mass shot tended to decrease. Therefore specific impulse and thrust efficiency had the same tendency as impulse bit. From this

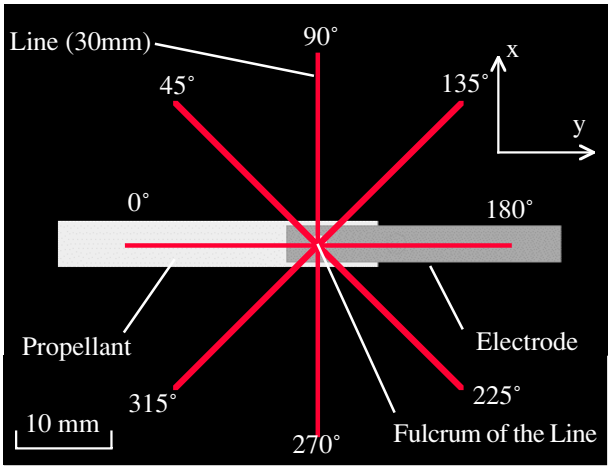

Fig.13 Experimental Apparatus of Self-induced Magnetic Field.

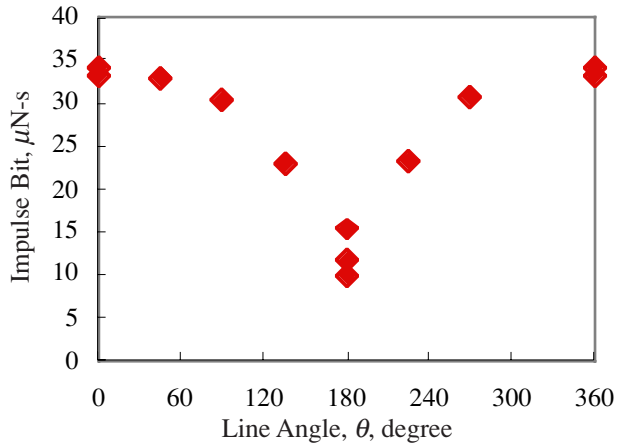

a) Impulse Bit vs. Line Angle.

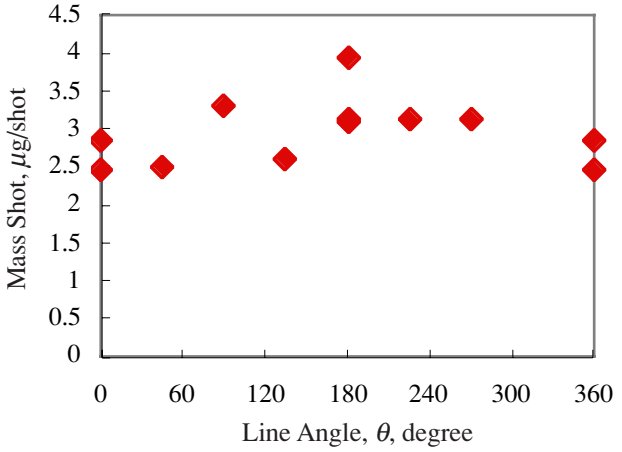

b) Mass Shot vs. Line Angle.

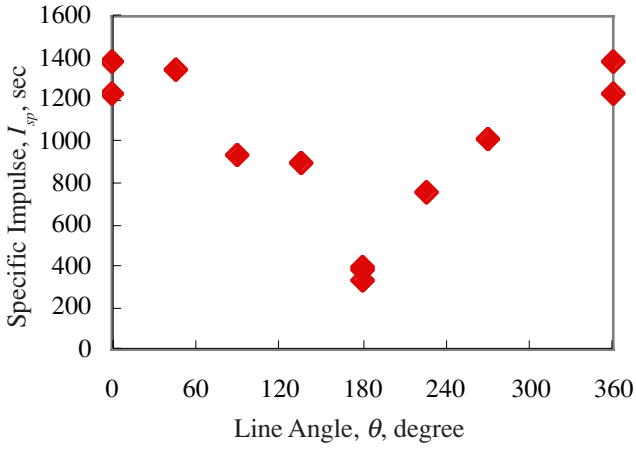

c) Specific Impulse vs. Line Angle.

Fig.14 The Performance with the Each Line Angle.

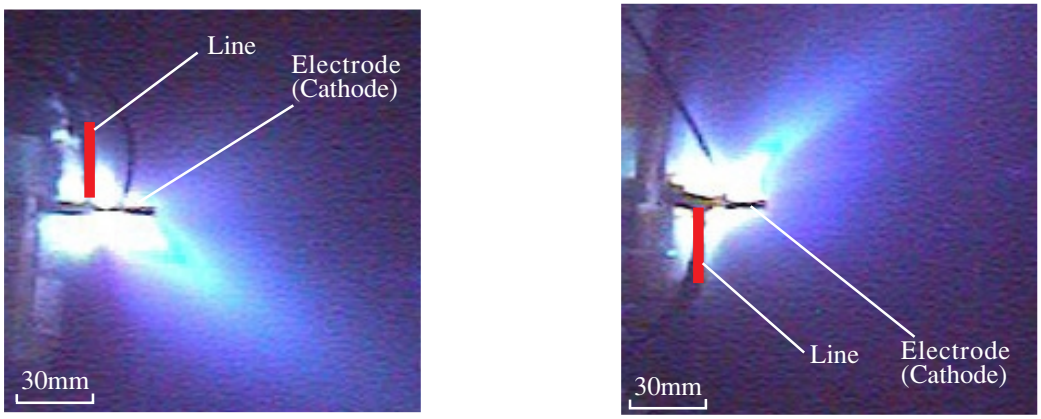

a) The Plume of 90˚ Line Angle. b) The Plume of 270˚ Line Angle.

Fig.15 The Photogragh of the Plume of 90˚ and 270˚ Line Angle.

result, where the angle of line was 0˚, impulse bit was the highest of all line angle operation because the plasma in the discharge chamber was accelerated faster than without the line effect. And where the angle of line was 180˚, mass shot was the highest because the plasma remained in the discharge chamber and impulse bit was the lowest because the self-induced magnetic field generated by the line and the main discharge were canceled each other. It means the $\boldsymbol{j} \times \boldsymbol{B}$ force decrease.

Figure 15 shows the plume with the 90˚, 270˚(-90˚) lines angle. As shown this figure, the plumes were inclined to the different direction. This phenomenon was the cause of self-induced magnetic field of the line. The direction of the magnetic field generated by the line was different from that generated by the main discharge current. This result shows the magnetic field of the line had an influence on that in the discharge chamber as the same with the result of the performance.

This result is needed to fix the configuration of the electrodes and the assembly of thruster. In the future, the phenomenon in the discharge chamber will investigate with high speed camera and the off-axis components of thrust will be measured with the target pendulum when the angle of line will be changed.

Conclusion

The plume characteristics of TMIT-PPT for μ-Lab Sat II were investigated. In the high speed camera experiment, we could observe the restrike and quasi-steady state of the discharge current. As a result of changing the hood angle, the performance of PPT with 0˚ hood is the lowest, compared with the other hood angles (15˚, 30˚, 45˚, 60˚ and without hood). It is the cause of the decrease of kinetic energy of the charged particle in the plume because of the collision with the hood wall. The performances of 15˚, 30˚, 45˚, 60˚ were approximately the same. In EM phase, we applied 30˚ hood. And, after 500,000 shots operation with 2.3 J/shot without hood, the aluminum plate 1100 mm away from the thruster were contaminated uniformly. However, the change of sample mass arranged on the aluminum plate was too small to measure. And, as a result of the preliminary inspection of the contamination, carbon was dominant and the proportion of the constituent elements were not different between near and far from the thrust axis. In the experiment to confirm the thrust direction of cant type thruster, the plume inclination was confirmed from the photograph, and thrust vector will be measured. As the result of changing the angle of line between thruster head and capacitor, as the angle of line increase, axial impulse bit had a tendency to decrease and mass shot had a tendency to increase. And the influence of the magnetic field was confirmed from the photograph. In the future, we will investigate the relation of line angle and thruster vector.

Acknowledgments

This work was supported in part by the Grant-in-Aid for Scientific Research (A) of Japan Society for the Promotion of Science. ULTRA 8 high speed camera was used in our experiments in cooperation with NAC Image Technology, Inc. The authors would like to acknowledge Ms. Miwa Igarashi (presently Mitsubishi Electric Engineering Co. Ltd.) who had developed the TMIT-PPT together with us in TMIT.

References

1. Kumagai. N, *et al*, "Research and Development Status of Low Power Pulsed Plasma Thruster System for μ-Lab Sat II," 28th International Electric Propulsion Conference, Toulouse, France, IEPC03-0202, 17-21 March 2003.

2. Tamura. K, *et al*, "Evaluation of Low Power Pulsed Thruster for μ-LabSat II," 38th Joint Propulsion Conference, Indianapolis, Indiana, USA, AIAA-2002-4272, July, 2002

3. Noda, A., *et al*, "Concept Design of μ-Lab Sat II," 44th Space Sciences and Technology Conference, Fukuoka, Japan, 00-3E13, 2000. (in Japanese)

4. Burton, R. L. and Turchi, P. J., "Pulsed Plasma Thruster," *Journal of Propulsion and Power 14*, *No. 5*, *716-735* September-October, 1998.

5. Rayburn, C., Campbell, M., "Development of a Micro Pulsed Plasma Thruster for the Dawgstar Nanosatellite," 36th Joint Propulsion Conference, Huntsville, Alabama, AIAA 2000-3256, 2000.

6. Hoskins, W. A. *et al*., "PPT Development Efforts at Primex Aerospace Company," 35th Joint Propulsion Conference, Los Angeles, California, USA, AIAA-99-2291, 1999.

7. Hirata, M., and Murakami, H., "Development of a Pulsed Plasma Engine," 17th International Electric Propulsion Conference, Tokyo, Japan, IEPC-84-48, 1984.

8. Benson, S. W., Arrington, L. A., Hoskins, W. A. and Meckel, N. J. "Development of a PPT for the EO-1 Spacecraft," 35th Joint Propulsion Conference, Los Angeles, California, USA, AIAA-99-2276, 1999.

9. William J. Guman, Martin Begun, "Exhaust Plume Studies of a Pulsed Plasma Thruster," 13th International Electric Propulsion Conference, San Diego, CA, AIAA 78-704, April 1978

10. Roger M. Myers, Lynn A. Arrinton, "Pulsed Plasma Thruster Contamination," 32nd Joint Propulsion Conference, Lake Buena Vista, FL, AIAA 96-2729, July, 1996

11. Dominic J. Palumbo, Martin Begun, "Plasma Acceleration in Pulsed Ablative Arc Discharges," Fairchild Industries Inc., AFOSR-TR-77-0623

12. Robert Vondra, *et al*, "A Pulsed Plasma Thruster for Satellite Control", Proceeding of the IEEE, Vol. 59, No.2, 1971, pp271-277

13. T. E. Markusic, E. Y. Choueiri, "Visualization of Current Sheet Canting in a Pulsed Plasma Accelerator," 26th International Electric Propulsion Conference, Kitakyushu, Japan, IEPC-99-206, October, 1999

14. Yanagi. R, Kimura. I, "A New Type Target for the Measurement of Impulse Bit of Pulsed Plasma Thrusters," AIAA-81-0712

15. Hirata. M, Murakami. H, "Exhaust Gas Analysis of a Pulsed Plasma Engine," 17th International Electric Propulsion Conference, Tokyo, Japan, IEPC-84-52, May, 1984